DisGUVery: a Versatile Open-source Software for High-throughput Image Analysis of Giant Unilamellar Vesicles

Lennard van Buren,[†] Gijsje Hendrika Koenderink,[*,†] and Cristina Martinez-Torres[*,†,‡]

†*Department of Bionanoscience, Kavli Institute of Nanoscience Delft, Delft University of Technology, 2629 HZ Delft, The Netherlands*

‡*Current address: Institute of Physics and Astronomy, University of Potsdam, 14476 Potsdam, Germany*

E-mail: g.h.koenderink@tudelft.nl; martineztorres@uni-potsdam.de

1 Supporting Information

1.1 Membrane analysis metrics

DisGUVery's membrane analysis modules Refined Membrane Detection (RMD) and Basic Membrane Analysis (BMA) support the use of different metrics (e.g. maximum intensity, mean intensity or sum intensity) to extract membrane fluorescence. This section should serve as a guide to choose the right metric according to the imaging source and research goal.

1.1.1 One-dimensional intensity profile

We consider a lipid bilayer membrane dyed with a fluorescent lipid. Since the membrane is thinner than the diffraction limit, the fluorescence intensity profile is given by the point spread function (PSF). We assume the PSF to be a Gaussian function, for a one-dimensional signal given by:

$$I(x) = Ae^{-\frac{(x-r)^2}{2\sigma^2}} \tag{1}$$

where x is the radial distance with respect to the GUV centre, r is the GUV radius, A is the amplitude of the signal and σ is the standard deviation, or the width of the point spread function. σ can be determined experimentally by fitting a Gaussian curve to the one-dimensional data.

In practice, fluorescence imaging is subjected to various sorts of noise (see fig. S6A). First, there is the camera read-out noise which contributes to a random noise in each pixel, $I_{cam}(x)$. Second, there is noise caused by out-of-focus fluorescence, ambient light and excitation light, which together add up to a minimum level of background fluorescence $I_{bg}(x)$. We split this background fluorescence in two contributions: a contribution $I_{bg,0}$ that is constant over the entire image, originating from e.g. excitation light and ambient light, and a varying contribution caused by out-of-focus fluorescence, $I_{bg,z}$. Considering the membrane signal

$I(x)$ of a particular GUV, the most dominant contribution to $I_{bg,z}$ comes from the out-of-focus membrane fluorescence of that GUV, which is high in the GUV interior and low outside the vesicle. We therefore write $I_{bg,z}$ as a Heavyside step function, with the interior out-of-focus fluorescence depending on the z-resolution of the system c (between 0 and 1, where 1 means good z-resolution, e.g. scanning confocal microscopy) as well as the amplitude of the membrane signal as:

$$I_{bg,z}(x) = \begin{cases} (1-c)A, & \text{if } x < r \\ 0, & \text{otherwise} \end{cases} \tag{2}$$

Summing up the membrane signal and noise contributions, we obtain the total signal:

$$I(x) = Ae^{-\frac{(x-r)^2}{2\sigma^2}} + I_{cam}(x) + I_{bg,0} + I_{bg,z}(x) \tag{3}$$

From the fluorescent signal, various metrics can be calculated with DisGUVery to report a membrane intensity. The membrane is first segmented by an inner radius r_{in} and an outer radius r_{out}. For a one-dimensional profile, the software can then obtain the sum of the signal $\sum(I(x))$ between r_{in} and r_{out}, given by:

$$\sum I(x) = NI_{bg,0} + \sum_{x=r_{in}}^{r_{out}} (Ae^{-\frac{(x-r)^2}{2\sigma^2}} + I_{cam}(x) + I_{bg,z}(x)))\Delta x \tag{4}$$

where Δx is the integration unit, typically the size of a pixel, and N is the total number of pixels over which is integrated, calculated from $N\Delta x = r_{out} - r_{in}$. The average signal $\overline{I}(x)$ can be calculated from eq. (4) by dividing over the number of pixels:

$$\overline{I}(x) = I_{bg} + \frac{1}{N} \sum_{x=r_{in}}^{r_{out}} (Ae^{-\frac{(x-r)^2}{2\sigma^2}} + I_{cam}(x) + I_{bg,z}(x))\Delta x \tag{5}$$

As can be seen from eq. (4) and eq. (5), both the total membrane intensity and average membrane intensity are influenced by the background signal I_{bg} and thus require background

subtraction. In addition, it is good to note that both the total and average intensity depend on the number of pixels used for integration. This means that the calculated intensity depends on the choice of r_{in} and r_{out}. Furthermore, it is good to consider that when N is small, e.g. when the membrane signal is narrow, white noise from I_{cam} can impact measured intensities. For larger N, e.g. in 2D-profiles, the effect of I_{cam} diminishes: $\sum_{x=0}^{N} I_{cam}(x) \to 0$.

Another descriptor that is often used to quantify membrane fluorescence is the maximum intensity. While the maximum intensity is a parameter that is easy to extract, its value is affected by pixelation and noise effects. For a continuous signal without noise, the maximum is simply given by the signal amplitude A. However, because of pixelation in the image, we do not measure the fluorescence intensity exactly at the membrane position, but at a position that is at maximum x_p separated from r, where x_p is the size of a pixel. For a signal without noise, the maximum intensity that is seen is given by:

$$I_{max} = Ae^{-\frac{x_p^2}{2\sigma^2}} \tag{6}$$

Consider using a 100x objective with a pixel size of $60nm$ and a PSF of $240nm$, and assume that σ is half the width of the PSF i.e. the width of the intensity peak is set by the PSF, then $I_{max} = 0.9A$. However, for a typical 10x objective with a pixel size of $600nm$ and a PSF of $1.2\mu m$, $I_{max} = 0.6A$. Pixel size can thus have a serious impact on the maximum intensity that is determined from a one-dimensional profile. Moreover, random noise in the image can affect the measured membrane position. Suppose that we have 20% noise (with respect to A), we can calculate the possible shift in membrane position Δx due to addition of this noise. The signal with noise is given by:

$$I(\Delta x) = Ae^{-\frac{\Delta x^2}{2\sigma^2}} + 0.2A \tag{7}$$

We then find the shift in membrane position by identifying the Δx for which $I(\Delta x) = A$, finally yielding $\Delta x = 0.6\sigma$. For a noise level of 50%, this yields $\Delta x = 1.2\sigma$. Assuming a σ

of 2 pixels, noise can cause a shift of one or two pixels dependent on the imaging settings.

1.1.2 Two-dimensional intensity profile

When considering the two-dimensional intensity profile, two other effects of pixelation must be taken into account.

First, angular slices must have a minimal thickness to extract pixel intensities from the slice (fig. S6B). While thinner slices approach one-dimensional intensity profiles, the slice thickness decreases when getting closer to the vesicle center. We compute the minimal angular separation θ where the slice thickness is larger than a pixel at a radial distance x. With the circle perimeter at a radial distance x given by $L = 2\pi x$, and the number of slices given by $N = 360/\theta$, the perimeter of an angular slice is $\Delta L = \frac{2\pi x}{N}$. For $\Delta L > 1$, we need $\theta > \frac{180}{\pi x}$. For a radial distance of 10 pixels, that is an angular separation of at least 6°. This effect is especially important for smaller vesicles or lower magnification images.

Second, the angular slice is drawn with four continuous lines, meaning that the edges of the mask run right through pixels(fig. S6C). This means that pixels that are partly outside the mask are weighed disproportionally into the average, while pixels partly inside the mask might be ignored. This effect is stronger for smaller slices. To get an idea of the number of pixels within the mask versus the number of pixels under the edge of the mask, we calculate the area and the perimeter of the angular mask. The area of the mask can be calculated by:

$$A_{slice} = \frac{\theta}{360}(A_{c,out} - A_{c,in}) \tag{8}$$

$$A_{slice} = \pi\frac{\theta}{360}(r_{out}^2 - r_{in}^2) \tag{9}$$

The perimeter, or the number of pixels at the borders of a slice can roughly be calculated by summing up the length of the four sides:

$$N_{edge} = 2(r_{out} - r_{in}) + \pi\frac{\theta}{360}(r_{out} + r_{in}) \tag{10}$$

Suppose we have a vesicle of $10\mu m$ radius. When imaged with an 100x objective with pixel size $60nm$ and a PSF of $240nm$, the membrane has an apparent thickness of 4 pixels, while the distance to the center of the vesicle is 150 pixels. Using an angular separation of 5 °and a total width of 12 pixels around the membrane, $r_{in} = 140$, $r_{out} = 160$, we obtain $A_{slice}/N_{edge} \sim 4$. This means that pixels at the edges have a relative small contribution, and thus that data can safely be extracted by integration. Problems arise when the size of the object in the image decreases. If we image the same vesicle with a 10x objective with pixel size $600nm$ and PSF $1.2\mu m$, we obtain a membrane width of 2 pixels and a radial distance of 15 pixels. Now, using a ring of 3 times the membrane width gives us $r_{in} = 12$ and $r_{out} = 18$, resulting in $A_{slice}/N_{edge} \sim 0.5$. Since edge pixels would weigh disproportionally large in this situation, it would be better to extract membrane intensities with one-dimensional extraction methods.

2 Supporting Figures

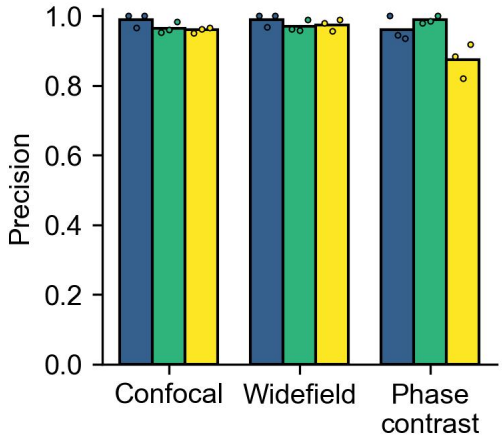

Figure S1: Precision of vesicle detection for different imaging types calculated from the same performance analysis results as shown in fig. 2G. Points represent results from individual human observers, bars represent the average values.

Table S1: Population sizes of vesicles in the different subcategories as counted by the four different observers in fig. 2H. The last column indicates the population size averaged over all observers.

Category	Observer 1	Observer 2	Observer 3	Observer 4	average
Standard	93	84	103	89	92
Edge	59	59	63	68	62
Unsharp	17	13	14	18	16
Anomalous	15	61	13	32	30

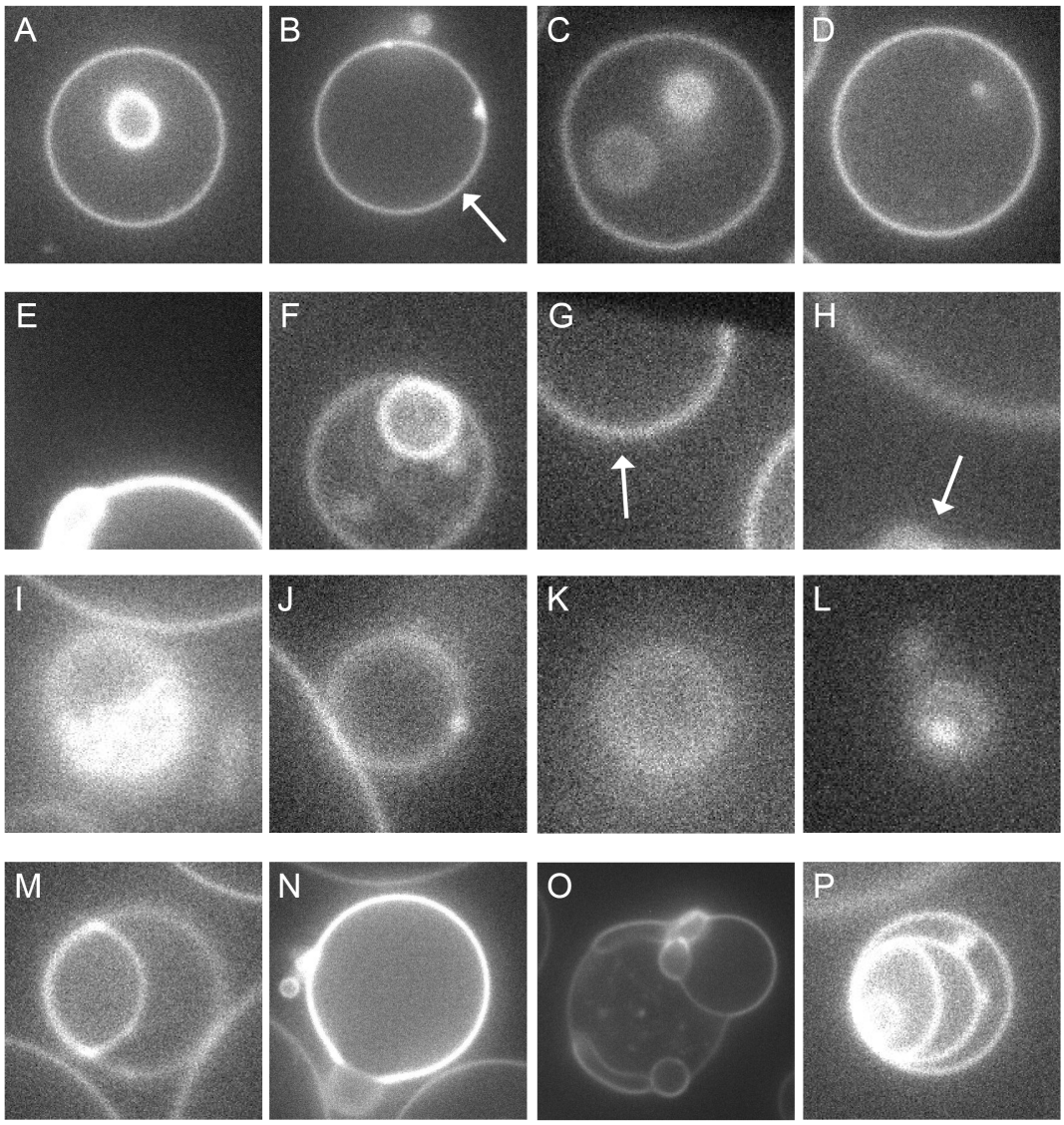

Figure S2: Gallery of example vesicles from different subcategories. In images containing multiple vesicles, the example vesicle has been indicated with an arrow. (A-D) Standard vesicles. (E-H) Vesicles at the edge of the image. (I-L) Vesicles that are out of focus. (M-P) Anomalous vesicles.

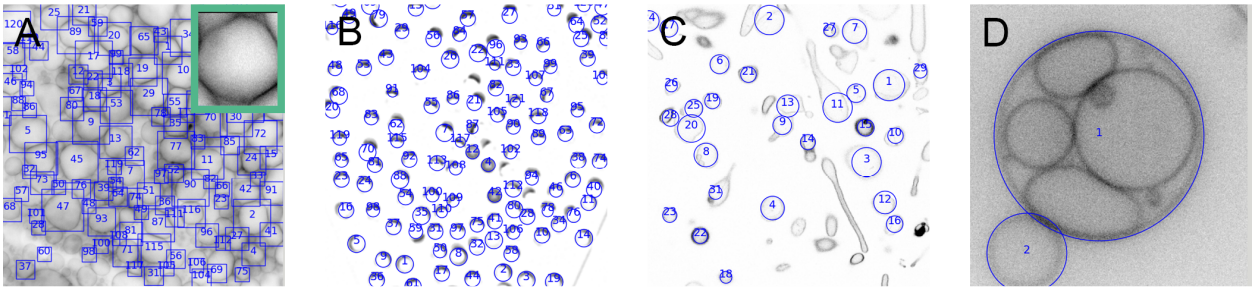

Figure S3: Applications of vesicle detection methods shown for the same input images as in manuscript fig. 3. (A) MTM detection in gel swelling experiment, (B) CHT detection in microfluidics, (C) CHT detection with deformed vesicles, (D) CHT detection with compartmentalized vesicles.

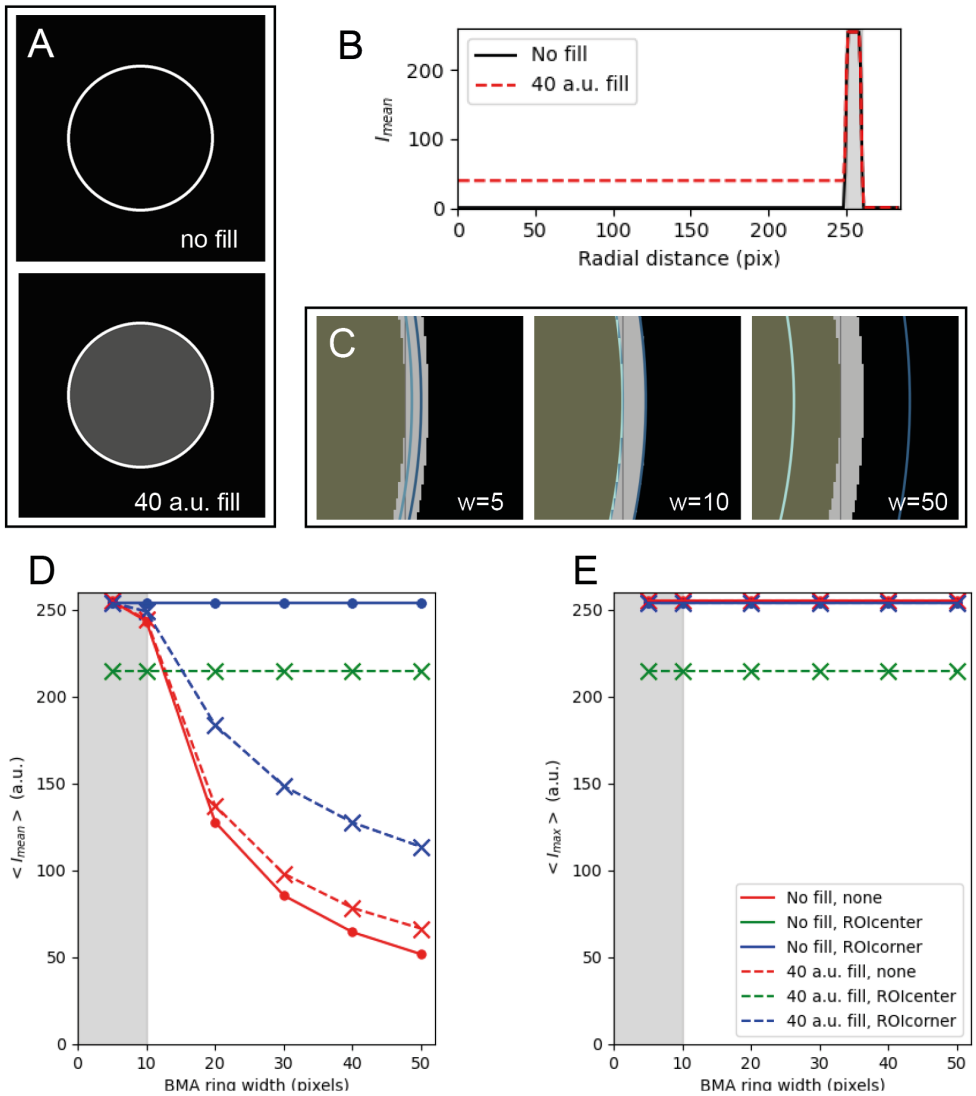

Figure S4: Influence of BMA ring width on intensity metrics. Synthetic images were created to map the effect of BMA width (w) and different background correction methods on membrane intensities extracted by DisGUVery. (A) Synthetic images with a radius of 250 pixels, membrane width of 10 pixels and confocal-like dark interior (upper) or widefield fluorescence-like lighter interior (bottom, fill of 40 a.u.) (B) Radial intensity profile obtained from both synthetic images. Greyed region is the membrane. (C) Zoom-in on BMA segmentation ring with width 5, 10 or 50 pixels, centred around the membrane middle. (D) Membrane mean intensity $< I_{mean} >$ extracted from the BMA ring by DisGUVery, averaged over 72 angular slices. For w larger than the membrane width (greyed region), $< I_{mean} >$ drops when no background correction is applied (red lines, see legend in panel E). This artefact is resolved by correcting with the pixel intensity in the vesicle centre (ROIcenter) which makes $< I_{mean} >$ independent of w (green lines). Correcting with the intensity in the corners of the bounding box confining the vesicle (ROIcorners) is useful when the vesicle interior has the same intensity as the outside (blue, solid vs dashed line). (E) Membrane maximum intensity I_{max} calculated similar to panel D, but from the maximum intensity in each angular slice. Here, in all cases the obtained intensity is independent of w.

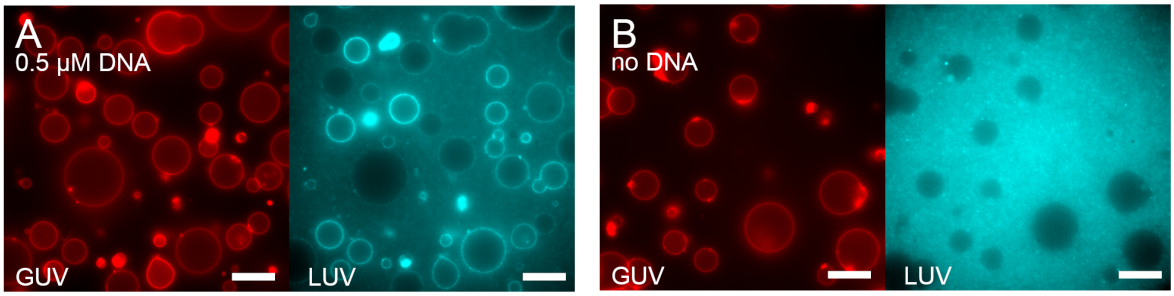

Figure S5: Binding of LUVs at different DNA concentrations. Images are epifluorescence images of Atto488 DOPE incorporated in the GUV membrane (red) and Atto 655 DOPE in the LUV membrane (cyan). Scale bar is 20 μm in all images. (A) At 0.5μM cholesterol-DNA, LUVs bound to the GUV membrane. (B) No membrane localization was observed in absence of cholesterol-DNA.

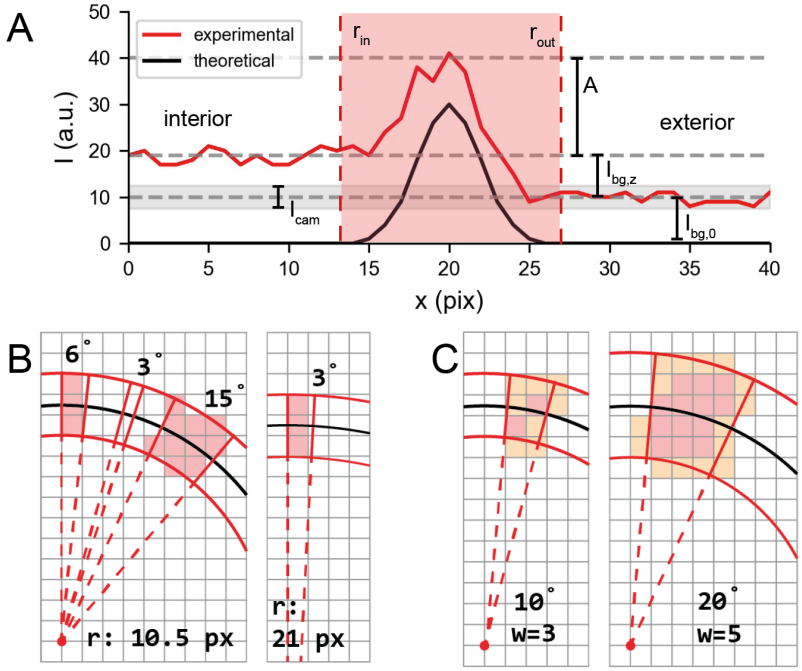

Figure S6: Experimental artefacts in membrane analysis. (A) Theoretical (black) and predicted experimental (red) one-dimensional membrane intensity profile of a GUV. The experimental profile is calculated with eq. (3) and eq. (2). While the theoretical profile is a simple Gaussian, the experimental profile is subjected to noise of various origins. Here, the radius $r = 20px$, $\sigma = 2px$, $A = 30$, $I_{cam} = 5$, confocality factor $c = 0.7$, and $I_{bg,0} = 10$. The red shaded part denotes the segmented area based on $r_{in} = 13$ and $r_{out} = 27$. (B,C) Discretisation effects in two-dimensional signal analysis. Segmentation lines are shown in red, the GUV membrane in black. (B) The apparent GUV size in the image imposes a minimum angular separation for integration. Integration should not be done with slices smaller than the pixel size. For a small GUV with a radius of 10.5 pixels, the minimum θ is 6°(left), while a more precise angular separation of 3° can be used for a vesicle twice as large (right). (C) Edge effects impact intensity analysis. Pixels located at the edge of the segmentation area (yellow pixels) are more prominent for smaller segmentation areas (left) as compared to larger regions (right). The size of the segmentation area is defined by the width of the ring as well as the angular separation.